Citation:
Hanif, H and Shafie, S and Jagun, ZT (2024) Maximizing thermal efficiency of a cavity using hybrid nanofluid. Journal of Cleaner Production, 441. pp. 1-8. ISSN 0959-6526 DOI: https://doi.org/10.1016/j.jclepro.2024.141089

Link to Leeds Beckett Repository record:
https://eprints.leedsbeckett.ac.uk/id/eprint/10536/

Document Version:
Article (Published Version)

Creative Commons: Attribution 4.0

© 2024 The Author(s).

The aim of the Leeds Beckett Repository is to provide open access to our research, as required by funder policies and permitted by publishers and copyright law.

The Leeds Beckett repository holds a wide range of publications, each of which has been checked for copyright and the relevant embargo period has been applied by the Research Services team.

We operate on a standard take-down policy. If you are the author or publisher of an output and you would like it removed from the repository, please contact us and we will investigate on a case-by-case basis.

Each thesis in the repository has been cleared where necessary by the author for third party copyright. If you would like a thesis to be removed from the repository or believe there is an issue with copyright, please contact us on openaccess@leedsbeckett.ac.uk and we will investigate on a case-by-case basis.

Journal of Cleaner Production 441 (2024) 141089

Contents lists available at ScienceDirect

Journal of Cleaner Production

journal homepage: www.elsevier.com/locate/jclepro

# Maximizing thermal efficiency of a cavity using hybrid nanofluid

Hanifa Hanif [a,b,*], Sharidan Shafie [b], Zainab Toyin Jagun [c,*]

[a] Department of Mathematics, Sardar Bahadur Khan Women's University, Quetta, Pakistan
[b] Department of Mathematical Sciences, Universiti Teknologi Malaysia, 81310 Johor Bahru, Johor, Malaysia
[c] Department of Real Estate, School of Built Environment, Engineering & Computing, Leeds Beckett University, NT212, Northern Terrace, City Campus, Leeds LS2 8AG, United Kingdom

ARTICLE INFO

Handling Editor: Panos Seferlis

*Keywords:*
Nanoscience
Heat transfer
Energy consumption
Finite difference method

ABSTRACT

**Background:** Increasing population growth and economic progress are partially to blame for the global issue of climate change and rising energy usage. One important step towards dealing with this issue would be to enhance the efficiency of a thermal system using tiny nanoparticles. Adding hybrid nanoparticles in a working fluid results in a "hybrid nanofluid" which can improve the efficiency of a thermal system to meet the rising demand for energy for current technology.

**Aim:** This study aims to increase the heat transfer in an inclined cavity using Ag–$TiO_2$ nanoparticles. The novel aspects of this research include evaluating the thermal performance of the suggested thermal system in the presence of a magnetic field and thermal radiation. Moreover, the heat transfer ability of a regular fluid, nanofluid, and hybrid nanofluid will also be compared with each other.

**Methodology:** The finite difference method is used to obtain the numerical solutions. The computations are done using MATLAB software.

**Findings:** The findings show that the applied magnetic field boosts the heat transfer capacity of nanoparticles. The heat transfer of the fluid increased by 1.6% and 2.5% on adding 4% vol. of $TiO_2$ and Ag–$TiO_2$ nanoparticles, respectively.

## 1. Introduction

Climate change and the increasing energy consumption in the world have become a worldwide issue, growing populations, and economic advancement are somehow responsible for this. Nano-materials may overcome these barriers due to their properties and nanoscale size (Hamzat et al., 2022; Hanif et al., 2024; Bratovcic, 2019; Hanif and Shafie, 2022c). However, these newly developing nanomaterials should have minimal operating costs because they will be used in areas with little infrastructure. Titanium oxide ($TiO_2$) is an ideal material in this context because it is photo-catalytically active, stable (in both acidic and basic environments), readily available, and nontoxic (Sanzone et al., 2018; Hovazi and Rostami, 2023; Hanif et al., 2023b). It is frequently utilized as a less expensive substitute for the standard industrial transparent conducting oxides. The primary concern with using titanium dioxide is its poor efficiency. Only 7% of solar energy can be used due to its broadband gap (3.2 eV), which results in low efficiency for solar-powered applications. Several alternative tactics have been attempted to maximize the efficiency of titanium dioxide consumption, one of which is combining $TiO_2$ with tiny silver Ag nanoparticles. Chakhtouna et al. (2021) discussed the significance of silver (Ag) nanoparticles in raising the Ag/$TiO_2$ photocatalysts' antibacterial activities. Transparent conducting oxide thin films are widely utilized in industry for a wide range of applications, including electrochromic devices and solar cells. In this regard, Dhar and Alford (2013) deposited the superior transparent $TiO_2$–Ag–$TiO_2$ composite electrode films by sputtering at ambient temperature on a substrate. Yu et al. (2011) claimed that the bactericidal activities of the synthesized Ag–$TiO_2$ thin films were higher than those of the plain $TiO_2$ nanofilm. Clinics and industries can use $TiO_2$ and Ag-deposited nanotubes for antibacterial purposes, especially because of their reusable nature (Li et al., 2013). Several authors discussed how the performance of $TiO_2$ can be enhanced by combining it with Ag nanoparticles (Hanif et al., 2023a; Chawhan et al., 2021; Soylu et al., 2022; Li et al., 2020). Keeping these environmentally friendly use of Ag and $TiO_2$ nanoparticles, this research is designed to analyze the significance of Ag–$TiO_2$ nanoparticles on the thermal efficiency of an energy-intensive system.

The wide range of engineering applications for convective heat transfer in thermal cavities, including heat exchangers, cooling electronics, fuel cells, geothermal power plants, food processing, and solar thermal systems, have made them highly sought-after. The mass–energy interaction between the surrounding and the moving fluid within a rectangular enclosure is known as convective heat transfer in a cavity.

* Corresponding authors.
*E-mail addresses:* hanifahanif@outlook.com (H. Hanif), z.t.jagun@leedsbeckett.ac.uk (Z.T. Jagun).

https://doi.org/10.1016/j.jclepro.2024.141089
Received 10 December 2023; Received in revised form 28 January 2024; Accepted 2 February 2024
Available online 3 February 2024
0959-6526/© 2024 The Author(s). Published by Elsevier Ltd. This is an open access article under the CC BY license (http://creativecommons.org/licenses/by/4.0/).

**Nomenclature**

**Roman letters**

| | |
|---|---|
| $(u, v)$ | Velocity components |
| $B_0$ | Magnetic field strength |
| $C_p$ | Specific heat capacity |
| $g$ | Gravitational acceleration |
| $k$ | Thermal conductivity |
| $k_b$ | Absorption parameter |
| $Nu$ | Nusselt number |
| $T$ | Temperature |
| $t$ | Time |
| Ec | Eckert number |
| M | Magnetic parameter |
| Pr | Prandtl number |
| Ra | Rayleigh number |
| Rd | Radiation parameter |

**Greek letters**

| | |
|---|---|
| $\beta_T$ | Volumetric thermal expansion |
| $\chi_1 - \chi_6$ | Nanofluid constants |
| $\Delta t$ | Time step |
| $\Delta x$ | Grid size in $x$ direction |
| $\Delta y$ | Grid size in $y$ direction |
| $\mu$ | Dynamic viscosity |
| $\nu$ | Kinematic viscosity |
| $\omega$ | Vorticity |
| $\psi$ | Stream function |
| $\rho$ | Density |
| $\sigma$ | Electrical conductivity |
| $\sigma_b$ | Stefan Boltzman parameter |
| $\varphi$ | Nanoparticles volume fraction |

**Subscripts/Superscripts**

| | |
|---|---|
| $(p_1, p_2)$ | Nanoparticles |
| $*$ | Non-dimensional |
| $f$ | Base fluid |
| $hnf$ | Hybrid nanofluid |
| $i$ | Grid point in $x$ direction |
| $j$ | Grid point in $y$ direction |
| $k$ | Time level |
| $nf$ | Nanofluid |

This interaction might be forced, mixed, or natural convection, depending on how the buoyancy and external forces are distributed (Hussien et al., 2021). The major efforts have been directed at improving the cavities' heat transport to fulfill the growing demand for engineering applications. Reddy et al. (2022) examined the behavior of multiwall carbon nanotubes (MWCNTs) in the fluid that was flowing in a square cavity with magnetic effects and detected that a 4% volume fraction of MWCNTs can improve the heat transfer rate by 7.2%. Turkyilmazoglu (2022a) investigated the fluid flow in a lid-driven cavity with a single lid divided into two distinct joint walls representing possible stirrers. Later, he extended his work to heat transfer analysis of the fluid flow inside a square cavity with a centrally located nonuniform heating wall (Turkyilmazoglu, 2022b). It was noticed that the heat transmission improved when an unevenly heated wall extended from the bottom to the top of the wall. The consequences of ternary nanoparticles ($Fe_3O_4$–MWCNTs–Cu) on the thermal performance of a cavity are investigated by Thirumalaisamy and Reddy (2023). They observed that the heat transfer rater increased by 3.4% on considering the $Fe_3O_4$–MWCNTs–Cu with the ratio 25:50:25 instead of 25:25:50. Selimefendigil and Chamkha (2021) analyzed the heat transfer characteristics of a square cavity containing a triangular-shaped segmented porous surface in the presence of Ag and MgO nanoparticles. They found that the average Nusselt number increased by 14.7% with 1% vol. fraction of Ag nanoparticles and 6.89% with 1% vol. fraction of MgO nanoparticles. Some interesting discussions on the significance of hybrid nanofluid inside a thermal system can be found in Hanif et al. (2022b), Acharya (2021), Giwa et al. (2020), Hanif and Shafie (2022a), Scott et al. (2022).

The magnetohydrodynamic (MHD) principle is significantly important in power generation, energy harvesting, pumping of materials, space transportation, astrophysical environments, and biomedical (Hanif and Shafie, 2022b; Ávalos-Zúñiga and Rivero, 2022; Seo and Ryu, 2023; Hanif et al., 2022a). The MHD system can potentially replace or supplement the traditional fossil fuel-based generating system, laying the groundwork for a completely sustainable society (Gupta et al., 2021). Many scientists have been interested in MHD fluid flow and heat transfer in a confined cavity considering the impact of natural convection due to its practical uses in cooling and heating applications (Mirzaei et al., 2023). The convective–radiative heat transfer of $Al_2O_3$–$CuO/H_2O$ flow in the presence of magnetic field is considered by Atashafrooz et al. (2023). According to their results, the maximum heat transfer rates were obtained in the absence of magnetic force with 3% $Al_2O_3$:3%CuO when radiative parameter ($Rd = 1$). Natural convection in MHD conjugate flow of a water-based nanofluid in an inclined cavity is discussed by Tasnim et al. (2023). The impact of nanoparticle shape on the natural convective heat transfer of a nanofluid in a wavy-walled cavity is investigated by Saha et al. (2023). According to their results, the heat transfer increased by 2.86% and 7.65% with spherical-shaped and blade-shaped nanoparticles, respectively. Tayebi and Chamkha (2020) investigated the consequences of the magnetic field on the irreversibility process in a square cavity using water-based Cu–$Al_2O_3$ hybrid nanofluid. Atashafrooz et al. (2020) discussed the interaction of magnetic field on heat transfer and entropy generation of $CuO/H_2O$ nanofluid flow in a trapezoidal recess. Atashafrooz (2020) analyzed the consequences of magnetic field and thermal radiation on the thermal behavior of $CuO/H_2O$ and $Al_2O_3/H_2O$ over an inclined step. Their findings indicate that the heat transfer rates are more impacted by CuO nanoparticles than by $Al_2O_3$ nanoparticles. Some good discussions on how a magnetic field affects the performance of a hybrid nanofluid in a cavity are given in Rashidi et al. (2021), Lawrence and Kumar (2021), Mansour et al. (2020), Roy (2022) and Sajjadi et al. (2018).

The aforementioned literature reveals that the convective heat transfer in thermal cavities is attracting the attention of researchers due to its broad applications in industry and science. Although several studies discussed heat transfer in thermal cavities, most of these studies considered steady cases where the time factor was ignored. However, some studies discussed the time-dependent convective heat transfer in cavities but those studies considered either regular fluid or mono nanofluids as a working fluid. It is important to mention that the desired heat transfer rates cannot be achieved using regular fluids due to their low thermal conductivity. The issue with mono nanofluids is that they either have high thermal efficiency or excellent physicochemical properties. A mono nanofluid does not have all of the needed properties for certain applications. To fill this research gap, the primary aim of this study is to examine an unsteady convective heat transfer in a square cavity and analyze how Ag–$TiO_2$/water hybrid nanofluid improves the thermal efficiency of a system. Furthermore, the addition of nanoparticles to the base fluid and the application of an external magnetic field can serve as both passive and active control mechanisms by regulating heat transmission in a thermal system (Geridonmez and

**Table 1**
Thermo-physical properties of nanoparticles and base fluid (Hanif et al., 2023a).

| Material | $\rho$ kg/m$^3$ | $\beta$ 1/K | $C_p$ J/kgK | $k$ W/mK | $\sigma$ S/m |
|---|---|---|---|---|---|
| Ag | 10 500 | 1.89$^{e-5}$ | 235 | 429 | 6.3e$^7$ |
| $TiO_2$ | 4250 | 0.9e$^{-5}$ | 686.2 | 8.9538 | 2.6e$^6$ |
| $H_2O$ | 997.1 | 21e$^{-5}$ | 4179 | 0.613 | 5.5e$^{-6}$ |

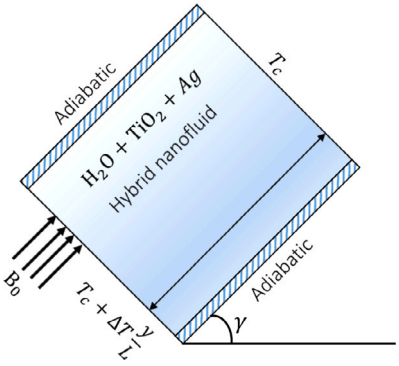


**Fig. 1.** Graphical representation.

Oztop, 2020). Therefore, this study also examines the impact of an external magnetic field on the thermal performance of the hybrid nanofluid in the presence of thermal radiation, which has not been studied before. The mathematical model comprised of the 2D coupled partial differential equations. A finite difference numerical technique is used to tackle the numerical solutions of the problem. It is important to note that solving the Navier–Stokes equations is a challenging task, and an analytical solution is not always available. Therefore, numerical approaches such as the finite difference method can be used to estimate the numerical solutions. The obtained numerical results are presented with the help of figures and tables.

## 2. Properties of Ag, $TiO_2$, and $H_2O$

Every material either fluid or solid has its own thermal properties; heat capacity, thermal expansion, and thermal conductivity; physical properties such as dynamic viscosity, density, and electrical conductivity. Table 1 illustrates these properties of silver $(Ag)$, titanium oxide $(TiO_2)$ and water $(H_2O)$.

## 3. Physical model

The natural convection of an incompressible hybrid nanofluid flow in an inclined square cavity with Rosseland heat flux is investigated in this work. The cavity is bounded by two adiabatic (horizontal) and two isothermal (vertical) walls. The left wall of the cavity is continuously heated with the temperature $T_c + \Delta T(y/L)$, while the right wall is kept at a constant temperature of $T_c$. Hybrid nanoparticles Ag–$TiO_2$ are added to the working fluid and a magnetic field is applied uniformly to the vertical axis. Moreover, the effects of Joule heating are also taken into account. Fig. 1 depicts the graphical representation of the mathematical model.

## 4. Mathematical model

The considered physical model is governed by the law of conservation of mass, momentum, and energy (Tasnim et al., 2023):

$$\frac{\partial u}{\partial x} + \frac{\partial v}{\partial y} = 0, \tag{1}$$

$$\rho_{hnf}\left(\frac{\partial u}{\partial t} + u\frac{\partial u}{\partial x} + v\frac{\partial u}{\partial y}\right) = -\frac{\partial p}{\partial x} + \mu_{hnf}\left(\frac{\partial^2 u}{\partial x^2} + \frac{\partial^2 u}{\partial y^2}\right) + g\left(\rho\beta_T\right)_{hnf}\left(T - T_c\right)\sin\gamma, \tag{2}$$

$$\rho_{hnf}\left(\frac{\partial v}{\partial t} + u\frac{\partial v}{\partial x} + v\frac{\partial v}{\partial y}\right) = -\frac{\partial p}{\partial y} + \mu_{hnf}\left(\frac{\partial^2 v}{\partial x^2} + \frac{\partial^2 v}{\partial y^2}\right) - \sigma_{hnf}B_0^2 v + g\left(\rho\beta_T\right)_{hnf}\left(T - T_c\right)\cos\gamma, \tag{3}$$

$$\left(\rho C_p\right)_{hnf}\left(\frac{\partial T}{\partial t} + u\frac{\partial T}{\partial x} + v\frac{\partial T}{\partial y}\right) = k_{hnf}\left(\frac{\partial^2 T}{\partial x^2} + \frac{\partial^2 T}{\partial y^2}\right) - \left(\frac{\partial q_{rx}}{\partial x} + \frac{\partial q_{ry}}{\partial y}\right) + \sigma_{hnf}B_0^2 v^2. \tag{4}$$

Initially, the fluid was at rest with wall temperature $T_c$, therefore, at $t \le 0$:

$$u = 0;\ v = 0;\ T = T_c. \tag{5}$$

The prescribed boundary conditions at $t > 0$ are:

$$\begin{aligned} &- \text{ all walls: } u = 0;\ v = 0,\\ &- \text{ horizontal walls: } \frac{\partial T}{\partial y} = 0,\\ &- \text{ left wall: } T = T_c + \Delta T\frac{y}{L},\\ &- \text{ at right wall: } T = T_c. \end{aligned} \tag{6}$$

The Rosseland approximation for the heat fluxes $q_{rx}$ and $q_{ry}$ in the energy Eq. (4) are given as Sivasankaran et al. (2020):

$$\frac{\partial q_{rx}}{\partial x} = -\frac{16\sigma_b T_c^3}{3k_b}\frac{\partial^2 T}{\partial x^2}, \quad \text{and} \quad \frac{\partial q_{ry}}{\partial y} = -\frac{16\sigma_b T_c^3}{3k_b}\frac{\partial^2 T}{\partial y^2}. \tag{7}$$

The physical and thermal properties of hybrid nanofluid; density $(\rho_{hnf})$, dynamic viscosity $(\mu_{hnf})$, thermal expansion $\left(\left(\rho\beta_T\right)_{hnf}\right)$, electrical conductivity $(\sigma_{hnf})$, heat capacity $\left(\left(\rho C_p\right)_{hnf}\right)$, and thermal conductivity $(k_{hnf})$ are presented as Hanif et al. (2023a):

$$\begin{aligned}
&\rho_{hnf} = \left(1-\varphi_{p_2}\right)\rho_{nf} + \varphi_{p_2}\rho_{p_2},\ \rho_{nf} = \left(1-\varphi_{p_1}\right)\rho_f + \varphi_{p_1}\rho_{p_1},\\
&\mu_{hnf} = \frac{\mu_f}{\left(1-\varphi_{p_1}\right)^{2.5}\left(1-\varphi_{p_2}\right)^{2.5}},\\
&\frac{\sigma_{hnf}}{\sigma_{nf}} = \frac{\left(\sigma_{p_2}+2\sigma_{nf}\right)+2\varphi_{p_2}\left(\sigma_{p_2}-\sigma_{nf}\right)}{\left(\sigma_{p_2}+2\sigma_{nf}\right)-\varphi_{p_2}\left(\sigma_{p_2}-\sigma_{nf}\right)},\\
&\frac{\sigma_{nf}}{\sigma_f} = \frac{\left(\sigma_{p_1}+2\sigma_f\right)+2\varphi_{p_1}\left(\sigma_{p_1}-\sigma_f\right)}{\left(\sigma_{p_1}+2\sigma_f\right)-\varphi_{p_1}\left(\sigma_{p_1}-\sigma_f\right)},\\
&\left(\rho\beta_T\right)_{hnf} = \left(1-\varphi_{p_2}\right)\left(\rho\beta_T\right)_{nf} + \varphi_{p_2}\left(\rho\beta_T\right)_{p_2},\\
&\left(\rho\beta_T\right)_{nf} = \left(1-\varphi_{p_1}\right)\left(\rho\beta_T\right)_f + \varphi_{p_1}\left(\rho\beta_T\right)_{p_1},\\
&\left(\rho C_p\right)_{hnf} = \left(1-\varphi_{p_2}\right)\left(\rho C_p\right)_{nf} + \varphi_{p_2}\left(\rho C_p\right)_{p_2},\\
&\left(\rho C_p\right)_{nf} = \left(1-\varphi_{p_1}\right)\left(\rho C_p\right)_f + \varphi_{p_1}\left(\rho C_p\right)_{p_1},\\
&\frac{k_{hnf}}{k_{nf}} = \frac{\left(k_{p_2}+2k_{nf}\right)+2\varphi_{p_2}\left(k_{p_2}-k_{nf}\right)}{\left(k_{p_2}+2k_{nf}\right)-\varphi_{p_2}\left(k_{p_2}-k_{nf}\right)},\\
&\frac{k_{nf}}{k_f} = \frac{\left(k_{p_1}+2k_f\right)+2\varphi_{p_1}\left(k_{p_1}-k_f\right)}{\left(k_{p_1}+2k_f\right)-\varphi_{p_1}\left(k_{p_1}-k_f\right)}.
\end{aligned} \tag{8}$$

Let us consider the following non-dimensional variables (Geridonmez and Oztop, 2020):

$$\begin{aligned}
&x^* = \frac{x}{L}, y^* = \frac{y}{L}, t^* = \frac{t\alpha_f}{L^2}, u^* = \frac{uL}{\alpha_f}, v^* = \frac{vL}{\alpha_f},\\
&T^* = \frac{T-T_c}{\Delta T}, p^* = \frac{pL^2}{\rho_f\alpha_f^2}, \psi^* = \frac{\psi}{\alpha_f}, \omega^* = \frac{\omega L^2}{\alpha_f}, \alpha_f = \frac{k_f}{\left(\rho C_p\right)_f}.
\end{aligned} \tag{9}$$

Before we proceed further, let us define the relationship of stream function $(\psi)$ and the vorticity $(\omega)$ with the velocity $(u, v)$:

$$u = \frac{\partial \psi}{\partial y},\ v = -\frac{\partial \psi}{\partial x},\ \omega = \frac{\partial v}{\partial x} - \frac{\partial u}{\partial y}. \tag{10}$$

Exploiting Eqs. (7)–(10) to the governing Eqs. (1)–(4) yields us to a set of non-dimensional equations (after removing '$*$'):

$$\frac{\partial^2 \psi}{\partial x^2} + \frac{\partial^2 \psi}{\partial y^2} = -\omega, \tag{11}$$

$$\frac{\chi_1}{Pr}\left(\frac{\partial \omega}{\partial t} + u\frac{\partial \omega}{\partial x} + v\frac{\partial \omega}{\partial y}\right) = \chi_2\left(\frac{\partial^2 \omega}{\partial x^2} + \frac{\partial^2 \omega}{\partial y^2}\right) - \chi_3 M\frac{\partial v}{\partial x} + \chi_4 Ra\left(\frac{\partial T}{\partial x}\cos\gamma - \frac{\partial T}{\partial y}\sin\gamma\right), \tag{12}$$

$$\chi_5\left(\frac{\partial T}{\partial t} + u\frac{\partial T}{\partial x} + v\frac{\partial T}{\partial y}\right) = \left(\chi_6 + Rd\right)\left(\frac{\partial^2 T}{\partial x^2} + \frac{\partial^2 T}{\partial y^2}\right) + \frac{\chi_3 M Ec}{Pr}v^2. \tag{13}$$

Here $\chi_1 - \chi_6$, $M$, $Rd$, $Pr$, $Ec$, and $Ra$ are the non-dimensional parameters defined as

$$\begin{aligned}
&\chi_1 = \frac{\rho_{hnf}}{\rho_f},\ \chi_2 = \frac{\mu_{hnf}}{\mu_f},\ \chi_3 = \frac{\sigma_{hnf}}{\sigma_f},\ \chi_4 = \frac{(\rho\beta_T)_{hnf}}{(\rho\beta_T)_f},\\
&\chi_5 = \frac{(\rho C_p)_{hnf}}{(\rho C_p)_f},\ \chi_6 = \frac{k_{hnf}}{k_f},\\
&M = \frac{\sigma_f B_0^2 L^2}{\mu_f},\ Rd = \frac{16\sigma_b T_c^3}{3k_b k_f},\ Pr = \frac{\nu_f}{\alpha_f},\\
&Ec = \frac{\nu_f^2}{\Delta T (C_p)_f L^2},\ Ra = \frac{g(\beta_T)_f \Delta T L^3}{\nu_f \alpha_f}.
\end{aligned} \tag{14}$$

The non-dimensional initial and boundary conditions are:

$$\begin{aligned}
&- \text{ all walls: } u = 0;\ v = 0;\ T = 0,\ \ t \le 0,\\
&- \text{ horizontal walls: } u = 0;\ v = 0,\ \ \frac{\partial T}{\partial y} = 0,\ \ t > 0,\\
&- \text{ left vertical wall: } u = 0;\ v = 0,\ \ T = y,\ \ t > 0,\\
&- \text{ right vertical wall: } u = 0;\ v = 0,\ \ T = 0,\ \ t > 0.
\end{aligned} \tag{15}$$

The Nusselt number on the left wall can be defined as:

$$Nu = -\chi_6\left(\frac{\partial T}{\partial x}\right)_{x=0}. \tag{16}$$

## 5. Numerical procedure

Let $\psi_{i,j}^k, \omega_{i,j}^k$, and $T_{i,j}^k$ be the numerical solutions of stream function, vorticity, and temperature at $(x_i, y_j, t_k)$, respectively. Given that $t_k = k\Delta t, k = 0, 1, \ldots, m, x_i = i\Delta x, i = 1, 2, \ldots, p, y_j = j\Delta y, j = 1, 2, \ldots, q$, where $\Delta t = t_f/m$ is the time step, $\Delta x = x_{max}/p$ is the mesh size along $x$-axis and $\Delta y = y_{max}/q$ is the mesh size along $y$-axis. Let $f$ be any general continuous function and $f_{i,j}^k$ be the numerical solution at $(x_i, y_j, t_k)$ then the forward difference for the time derivative and the central difference for the spatial derivatives are given as (Hanif, 2021a,b, 2022):

- time derivative

$$\frac{\partial f}{\partial t}(x_i, y_j, t_k) \simeq \frac{f_{i,j}^{k+1} - f_{i,j}^k}{\Delta t}. \tag{17}$$

- spatial first-order derivatives

$$\frac{\partial f}{\partial x}(x_i, y_j, t_k) \simeq \frac{f_{i+1,j}^k - f_{i-1,j}^k}{2\Delta x},\ \text{ and }\ \frac{\partial f}{\partial y}(x_i, y_j, t_k) \simeq \frac{f_{i,j+1}^k - f_{i,j-1}^k}{2\Delta y}. \tag{18}$$

- spatial second-order derivatives

$$\frac{\partial^2 f}{\partial x^2}(x_i, y_j, t_k) \simeq \frac{f_{i+1,j}^k - 2f_{i,j}^k + f_{i-1,j}^k}{\Delta x^2},\ \text{ and }\ \frac{\partial^2 f}{\partial y^2}(x_i, y_j, t_k) \simeq \frac{f_{i,j+1}^k - 2f_{i,j}^k + f_{i,j-1}^k}{\Delta y^2}. \tag{19}$$

Using the aforementioned time and spatial derivatives in Eqs. (11)–(13) and rearranging the resultant equations lead us to:

$$\psi_{i,j}^{k+1} \approx \omega_{i,j}^k + \mathcal{L}_{i,j}^{k+1}[\psi] + \mathcal{U}_{i,j}^k[\psi]. \tag{20}$$

$$\omega_{i,j}^{k+1} \approx \omega_{i,j}^k + C_{i,j}^k[\omega] + \mathcal{M}_{i,j}^k[\psi] + \mathcal{B}_{i,j}^k[T]. \tag{21}$$

$$T_{i,j}^{k+1} \approx T_{i,j}^k + \mathcal{D}_{i,j}^k[T] + \mathcal{J}_{i,j}^k[\psi]. \tag{22}$$

Here, $\mathcal{B}, C, \mathcal{D}, \mathcal{J}, \mathcal{L}, \mathcal{M}$, and $\mathcal{U}$ are the vectors of order $(p+1)\times 1$ for each $j$. A code has been developed in MATLAB to find the numerical solutions of $\psi, \omega$, and $T$ at time $t = k+1$. The computations have been started using the initial conditions and the iterations are repeated until the tolerance rate is achieved:

$$\left|\frac{\varpi^{k+1} - \varpi^k}{\varpi^k}\right| \le 10^{-5}, \tag{23}$$

where $\varpi$ represents a component of a general solution. Note that the considered numerical scheme is conditionally stable.

## 6. Results and discussion

The numerical findings for the convective heat transfer of a hybrid nanofluid in an inclined square cavity with a transverse magnetic field are provided and analyzed in this section. The governing factors for this study are nanoparticle volume fraction $\varphi$, Rayleigh number $Ra$, magnetic parameter $M$, thermal radiation $Rd$, and Eckert number $Ec$. Table 2 illustrates the comparison of the Nusselt number with the results of previous studies.

In Fig. 2, typical streamlines and isotherms are illustrated for two different values of Rayleigh number $Ra = 10^3$ and $Ra = 10^4$. The buoyancy-driven circulation flows within the cavity are noticeable due to the change in Rayleigh number and magnetic parameter. The magnitude of these circulations grows with the increasing Rayleigh number and lowers in the presence of the magnetic field. This is due to the buoyancy forces which grow stronger with Rayleigh number and overcome the viscosity forces. Moreover, the isotherms indicate that the average fluid temperature within the cavity rises, as does the flow obstruction caused by Lorentz force. The magnetic field creates drag-like forces known as the Lorentz force. These resistive forces, in turn, raise the temperature. As the magnetic parameter $M$ increases, the Lorentz force grows. The fluctuations in the isotherms are more dominant for the higher value of $Ra$. In Fig. 3, the isotherms and streamlines are illustrated for four different cases; (i) $Rd = 0$ and $M = 0$, (ii) $Rd = 0$, and $M = 10$, (iii) $Rd = 2$ and $M = 0$, and (iv) $Rd = 2$ and $M = 10$. The results show that the amplitude of these flows is maximum in the absence of the magnetic field. It is also demonstrated that the radiation impacts are mostly felt on the streamlines in the center of the cavity, where the flow is least strong. The isotherms move away from the heated wall when a magnetic field is applied in either $Rd = 0$ or $Rd = 2$. This is because of resistive Lorentz forces that are generated due to the magnetic field. The isotherm lines are curvier when $Rd = 0$ and $M = 0$. Furthermore, the average fluid temperature increases when Rosseland's heat flux is applied in horizontal and vertical directions, and the maximum temperature is observed in the presence of a magnetic field when $Rd = 2$. The effects of Eckert number on the fluid flow and the temperature are depicted in Fig. 4. Eckert number is described as the kinetic energy to enthalpy driving force ratio in heat transfer. The findings show that the streamlines tend to move towards the center when the Eckert number increases, indicating that the viscous dissipation effects are dominating. The existence of viscous

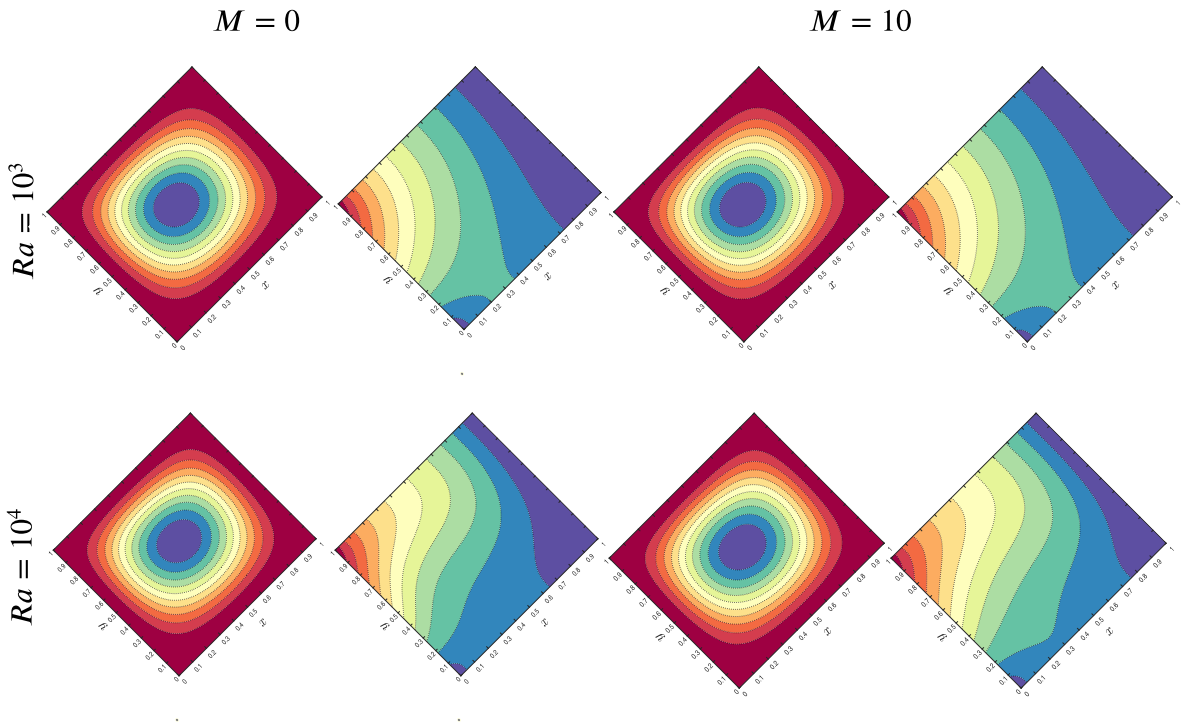


**Fig. 2.** Streamlines and isotherms against $Ra$.

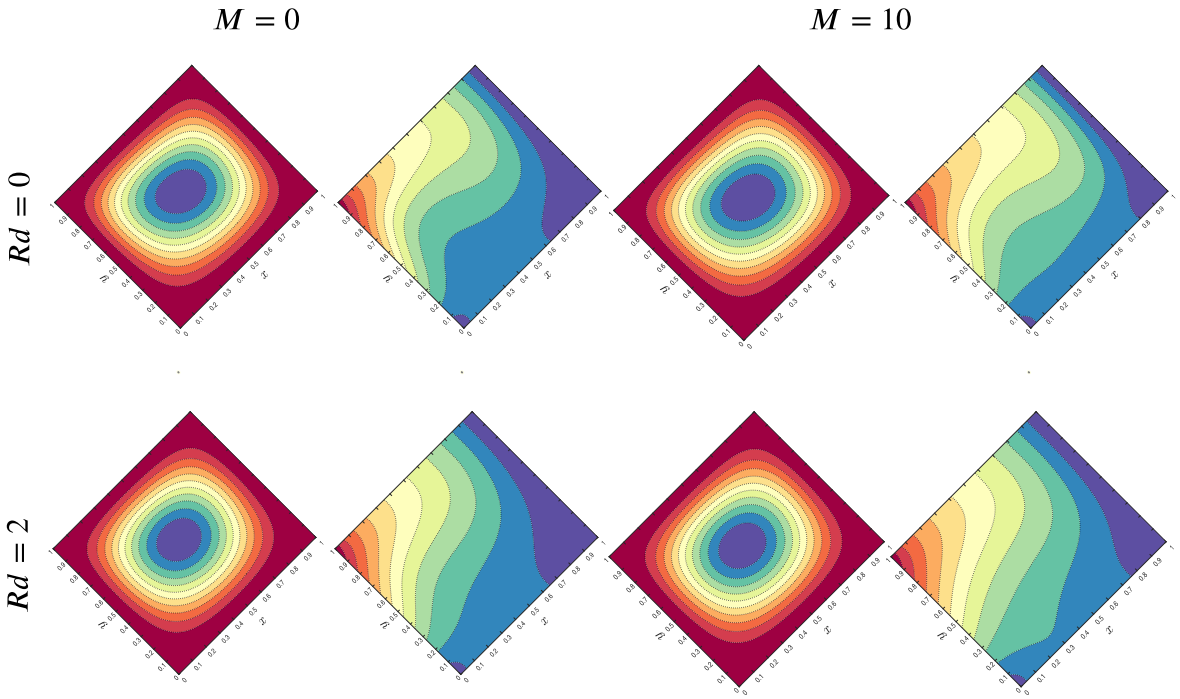


**Fig. 3.** Streamlines and isotherms against $Rd$.

**Table 2**
Comparison of $Nu$ with previous studies.

| $Ra$ | Geridonmez and Oztop (2020) | Khanafer et al. (2003) | de Vahl Davis (1983) | Present |
|---|---|---|---|---|
| $Ra = 10^3$ | 1.118 | 1.118 | 1.118 | 1.1197 |
| $Ra = 10^4$ | 2.246 | 2.245 | 2.243 | 2.4401 |
| $Ra = 10^5$ | 4.518 | 4.522 | 4.519 | 4.5109 |
| $Ra = 10^6$ | 8.810 | 8.826 | 8.799 | 8.8031 |

**Table 3**
Heat transfer rates of $TiO_2/H_2O$ and Ag–$TiO_2/H_2O$ with different values of $\varphi$ and $Ec$.

| $\varphi$ | $TiO/H_2O$ | | | Ag–$TiO/H_2O$ | | |
|---|---|---|---|---|---|---|
| | $Ec = 0.005$ | $Ec = 0.008$ | $Ec = 0.01$ | $Ec = 0.005$ | $Ec = 0.008$ | $Ec = 0.01$ |
| 0 | 1.0889 | 0.98236 | 0.91186 | 1.0889 | 0.98236 | 0.91186 |
| 0.02 | 1.0924 | 0.98794 | 0.91896 | 1.0992 | 0.99283 | 0.92259 |
| 0.04 | 1.0952 | 0.99388 | 0.92673 | 1.1093 | 1.004 | 0.93416 |

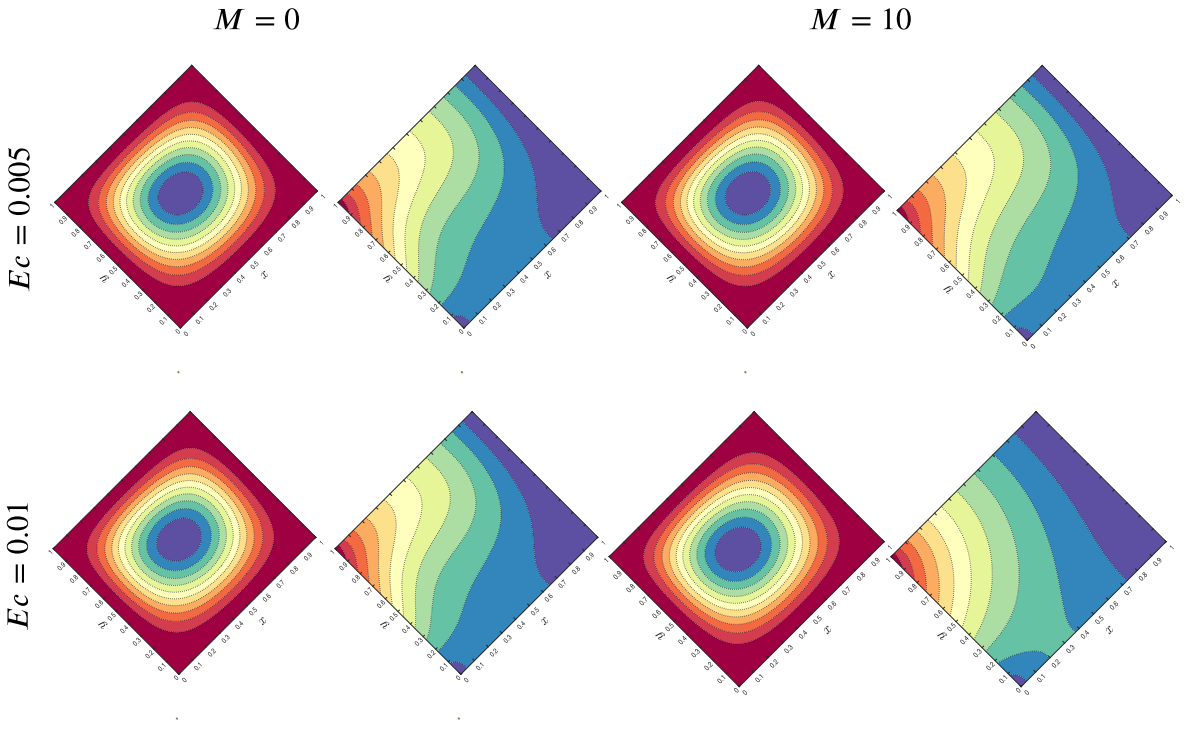


**Fig. 4.** Streamlines and isotherms against $Ec$.

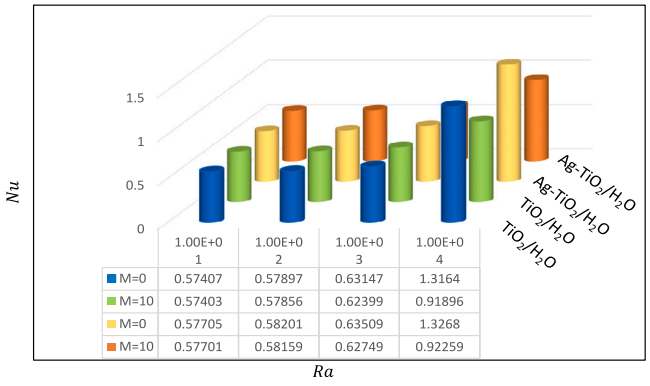


**Fig. 5.** Nusselt number against $Ra$.

dissipation has a substantial influence at the top-left and bottom-right corners with high flow velocities. Furthermore, the temperature rises when the Eckert number rises. The Eckert number is generated due to Joule heating, therefore, it does not have any effect When $M = 0$.

The consequences of Rayleigh number $Ra$ on heat transfer rates of $TiO_2/H_2O$ nanofluid and Ag–$TiO_2/H_2O$ hybrid nanofluid are drawn in Fig. 5. Two different cases are considered: (i) without magnetic field ($M = 0$), and (ii) with magnetic field ($M = 10$). The results show that the heat transfer rates increased with the increasing values of $Ra$ in both cases i.e., $M = 0$ and $M = 10$. Augmentation of Ra leads to increased circulation and convective energy transmission. There are several ways in which increasing heat transfer rates might benefit the environment. For example, increasing the efficiency of a thermal system can aid in lowering energy usage. This can thus result in a reduced carbon footprint and a decrease in greenhouse gas emissions. In Fig. 6, the heat transfer rates of $TiO_2/H_2O$ nanofluid and Ag–$TiO_2/H_2O$ hybrid nanofluid are depicted for different values of $Rd$ and $M$. It is found that the heat transfer rates are minimal when Rosseland's heat fluxes are applied to the system. Nusselt number decreases as the radiation parameter is increased because it modifies the isothermal lines (Fig. 3). However, maximum heat transfer rates are obtained when tiny Ag nanoparticles are added to $TiO_2/H_2O$. When $Rd = 0$, the heat transfer rates increased 0.5% on adding $Ag$ nanoparticles to the fluid and the increment was 0.8% when thermal radiation was applied ($Rd = 2$).

In Table 3, the heat transfer rates are presented for different nanoparticle concentrations $\varphi = 0\%, 2\%, 4\%$. It is evident from the results that the thermal efficiency of the cavity increases with increasing nanoparticle volume concentrations. This was expected since the thermal conductivity of nanoparticles is much higher than the thermal conductivity of a regular base fluid. As a result, increasing the concentration of nanoparticles in a base fluid eventually elevates the heat transfer rates. Here $\varphi = 0$ corresponds to the regular base fluid which is pure water. Moreover, the effects of the Eckert number are also examined and it is found that the heat transfer rate decreases due to the viscous dissipation. However, maximum heat transfer rates are attained by the fluid with Ag–$TiO_2/H_2O$ hybrid nanofluid compared to $TiO_2/H_2O$. The heat transfer of hybrid nanofluid is 2.5% and 0.8% greater compared to pure water and nanofluid, respectively. Table 4 illustrates the heat transfer rates for different cases of the magnetic field $M = 0, 5, 10$ for different fluids (i) pure water (ii) nanofluid,

**Table 4**
Heat transfer rates of $H_2O$, $TiO_2/H_2O$ and $Ag–TiO_2/H_2O$ with different values of $M$ and $Ec$.

| $M$ | $H_2O$ | | $TiO/H_2O$ | | $Ag–TiO/H_2O$ | |
|---|---|---|---|---|---|---|
| | $Ec = 0.005$ | $Ec = 0.01$ | $Ec = 0.005$ | $Ec = 0.01$ | $Ec = 0.005$ | $Ec = 0.01$ |
| 0 | 1.315 | 1.315 | 1.3164 | 1.3164 | 1.3268 | 1.3268 |
| 5 | 1.1947 | 1.0987 | 1.1968 | 1.1027 | 1.2053 | 1.1094 |
| 10 | 1.0889 | 0.91186 | 1.0924 | 0.91896 | 1.0992 | 0.92259 |

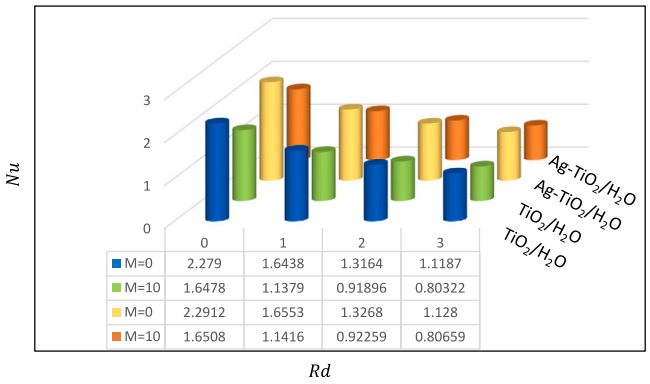


**Fig. 6.** Nusselt number against $Rd$.

and (iii) hybrid nanofluid. It is shown that the maximum heat transfer rates are obtained when magnetic effects are minimal. Likewise, heat transfer rates are decreased when Eckert number grows. However, these limitations can be overcome by adding tiny nanoparticles to the fluid. In the presence of the magnetic field, the heat transfer rates increased up to 0.8% and 1.2% on adding 2% vol. fraction of $TiO_2$ nanoparticles and $Ag–TiO_2$ hybrid nanoparticles in water-based fluid, respectively. When $M = 0$, the heat transfer increased up to 0.1% and 0.9% due to $TiO_2$ and $Ag–TiO_2$, respectively. These results showed that the effects of nanoparticles are more significant in the presence of a magnetic field.

## 7. Conclusions

This research aimed to minimize the energy consumption by increasing the thermal performance of a cavity using nanoparticles. In this regard, a hybrid nanofluid is prepared by adding tiny Ag and $TiO_2$ nanoparticles in water-based fluid. Meanwhile, the consequences of magnetic field, thermal radiation, and Joule heating are also examined. The 2D mathematical model was analyzed using a finite difference numerical approach. The key findings of the research are:

- The buoyancy-driven circulation flow within the cavity is noticeable due to the change in Rayleigh number and magnetic parameter.
- The fluid temperature is increased significantly when a magnetic field is applied in the presence of thermal radiation.
- The heat transfer rates increased up to 2.5% and 1.6% with 4% vol. of $Ag–TiO_2$ and $TiO_2$, respectively.
- The heat transfer capability of nanoparticles is enhanced when the magnetic field is applied.
- Addition of Ag in $TiO_2/H_2O$ nanofluid increased the heat transfer rates by 0.2% without thermal radiation and 0.4% when the thermal radiation is applied.

The influence of the hybrid nanofluid can significantly increase the thermal performance of a cavity which is vitally important in solar thermal systems, heat exchangers, cooling/heating of buildings, thermal energy storage systems, geothermal systems, and food processing. There are several other ways in which the increasing heat transfer rates might benefit the environment. For example, increasing the efficiency of a thermal system can aid in lowering energy usage. This can thus result in a reduced carbon footprint and greenhouse gas emissions. Besides the advantages, there are some limitations to adding nanoparticles in a base fluid. For example, the overall performance of the system may be hampered by the fluid's stability and sedimentation.

## CRediT authorship contribution statement

**Hanifa Hanif:** Writing – original draft, Software, Methodology, Investigation, Formal analysis, Conceptualization. **Sharidan Shafie:** Supervision, Resources. **Zainab Toyin Jagun:** Resources, Conceptualization.

## Declaration of competing interest

The authors declare that they have no known competing financial interests or personal relationships that could have appeared to influence the work reported in this paper.

## Data availability

No data was used for the research described in the article.

## Acknowledgment

The authors would like to acknowledge the financial support from Universiti Teknologi Malaysia for the funding under UTM Fundamental Research (UTMFR: Q.J130000.3854.23H22).

## Funding

No funding was received.

## References

Acharya, N., 2021. On the flow patterns and thermal control of radiative natural convective hybrid nanofluid flow inside a square enclosure having various shaped multiple heated obstacles. Eur. Phys. J. Plus 136 (8), 889. http://dx.doi.org/10.1140/epjp/s13360-021-01892-0.

Atashafrooz, M., 2020. Influence of radiative heat transfer on the thermal characteristics of nanofluid flow over an inclined step in the presence of an axial magnetic field. J. Therm. Anal. Calorim. 139 (5), 3345–3360. http://dx.doi.org/10.1007/s10973-019-08672-0.

Atashafrooz, M., Sajjadi, H., Delouei, A.A., 2020. Interacting influences of Lorentz force and bleeding on the hydrothermal behaviors of nanofluid flow in a trapezoidal recess with the second law of thermodynamics analysis. Int. Commun. Heat Mass Transfer 110, 104411. http://dx.doi.org/10.1016/j.icheatmasstransfer.2019.104411.

Atashafrooz, M., Sajjadi, H., Delouei, A.A., 2023. Simulation of combined convective-radiative heat transfer of hybrid nanofluid flow inside an open trapezoidal enclosure considering the magnetic force impacts. J. Magn. Magn. Mater. 567, 170354. http://dx.doi.org/10.1016/j.jmmm.2023.170354.

Ávalos-Zúñiga, R.A., Rivero, M., 2022. Theoretical modeling of a vortex–type liquid metal MHD generator for energy harvesting applications. Sustain. Energy Technol. Assess. 52, 102056. http://dx.doi.org/10.1016/j.seta.2022.102056.

Bratovcic, A., 2019. Different applications of nanomaterials and their impact on the environment. SSRG Int. J. Mater. Sci. Eng. 5 (1), 1–7.

Chakhtouna, H., Benzeid, H., Zari, N., Qaiss, A.e.K., Bouhfid, R., 2021. Recent progress on $Ag/TiO_2$ photocatalysts: Photocatalytic and bactericidal behaviors. Environ. Sci. Pollut. Res. 28, 44638–44666. http://dx.doi.org/10.1007/s11356-021-14996-y.

Chawhan, S.S., Barai, D.P., Bhanvase, B.A., 2021. Investigation on thermophysical properties, convective heat transfer and performance evaluation of ultrasonically synthesized Ag-doped $TiO_2$ hybrid nanoparticles based highly stable nanofluid in a minichannel. Therm. Sci. Eng. Prog. 25, 100928. http://dx.doi.org/10.1016/j.tsep.2021.100928.

de Vahl Davis, G., 1983. Natural convection of air in a square cavity: A bench mark numerical solution. Int. J. Numer. Methods Fluids 3 (3), 249–264. http://dx.doi.org/10.1002/fld.1650030305.

Dhar, A., Alford, T., 2013. High quality transparent $TiO_2$/Ag/$TiO_2$ composite electrode films deposited on flexible substrate at room temperature by sputtering. APL Mater. 1 (1), http://dx.doi.org/10.1063/1.4808438.

Geridonmez, B.P., Oztop, H., 2020. MHD natural convection in a cavity in the presence of cross partial magnetic fields and $Al_2O_3$–water nanofluid. Comput. Math. Appl. 80 (12), 2796–2810. http://dx.doi.org/10.1016/j.camwa.2020.10.003.

Giwa, S.O., Sharifpur, M., Meyer, J.P., 2020. Experimental study of thermo–convection performance of hybrid nanofluids of $Al_2O_3$-MWCNT/water in a differentially heated square cavity. Int. J. Heat Mass Transfer 148, 119072. http://dx.doi.org/10.1016/j.ijheatmasstransfer.2019.119072.

Gupta, J., Singla, M.K., Nijhawan, P., 2021. Magnetohydrodynamic system—A need for a sustainable power generation source. Magnetohydrodynamics 57 (2), 251–272. http://dx.doi.org/10.22364/mhd.57.2.9.

Hamzat, A.K., Omisanya, M.I., Sahin, A.Z., Oyetunji, O.R., Olaitan, N.A., 2022. Application of nanofluid in solar energy harvesting devices: A comprehensive review. Energy Convers. Manage. 266, 115790. http://dx.doi.org/10.1016/j.enconman.2022.115790.

Hanif, H., 2021a. Cattaneo–Friedrich and Crank–Nicolson analysis of upper-convected Maxwell fluid along a vertical plate. Chaos Solitons Fractals 153, 111463. http://dx.doi.org/10.1016/j.chaos.2021.111463.

Hanif, H., 2021b. A finite difference method to analyze heat and mass transfer in kerosene based $\gamma$-oxide nanofluid for cooling applications. Phys. Scr. 96 (9), 095215. http://dx.doi.org/10.1088/1402-4896/ac098a.

Hanif, H., 2022. A computational approach for boundary layer flow and heat transfer of fractional Maxwell fluid. Math. Comput. Simulation 191, 1–13. http://dx.doi.org/10.1016/j.matcom.2021.07.024.

Hanif, H., Khan, A., Rijal Illias, M., Shafie, S., 2024. Significance of Cu-$Fe_3O_4$ on fractional Maxwell fluid flow over a cone with Newtonian heating. J. Taibah Univ. Sci. 18 (1), 2285491. http://dx.doi.org/10.1080/16583655.2023.2285491.

Hanif, H., Lund, L.A., Shafie, S., 2023a. Dynamics of Ag-$TiO_2$/$H_2O$ between two coaxial cylinders: A computational approach. Eur. Phys. J. Plus 138 (12), 1153. http://dx.doi.org/10.1140/epjp/s13360-023-04802-8.

Hanif, H., Shafie, S., 2022a. Application of Cattaneo heat flux to Maxwell hybrid nanofluid model: A numerical approach. Eur. Phys. J. Plus 137 (8), 989. http://dx.doi.org/10.1140/epjp/s13360-022-03209-1.

Hanif, H., Shafie, S., 2022b. Impact of $Al_2O_3$ in electrically conducting mineral oil-based Maxwell nanofluid: Application to the petroleum industry. Fractal Fract. 6 (4), 180. http://dx.doi.org/10.3390/fractalfract6040180.

Hanif, H., Shafie, S., 2022c. Interaction of multi–walled carbon nanotubes in mineral oil based Maxwell nanofluid. Sci. Rep. 12 (1), 1–16. http://dx.doi.org/10.1038/s41598-022-07958-y.

Hanif, H., Shafie, S., Chamkha, A., 2022a. Effect of Ohmic heating on magnetohydrodynamic flow with variable pressure gradient: A computational approach. Waves Random Complex Media 1–16. http://dx.doi.org/10.1080/17455030.2022.2141916.

Hanif, H., Shafie, S., Jagun, Z., 2023b. Maximizing heat transfer and minimizing entropy generation in concentric cylinders with CuO-MgO-$TiO_2$ nanoparticles. Chinese J. Phys. http://dx.doi.org/10.1016/j.cjph.2023.12.021.

Hanif, H., Shafie, S., Roslan, R., Ali, A., 2022b. Collision of hybrid nanomaterials in an upper–convected Maxwell nanofluid: A theoretical approach. J. King Saud Univ.-Sci. 102389. http://dx.doi.org/10.1016/j.jksus.2022.102389.

Hovazi, E., Rostami, E., 2023. Fabrication, characterization, and biological applications of $TiO_2$ nanoparticles coated by chitosan. Nanomed. Res. J. 8 (1), 50–60. http://dx.doi.org/10.22034/NMRJ.2023.01.005.

Hussien, A.A., Al-Kouz, W., El Hassan, M., Janvekar, A.A., Chamkha, A.J., 2021. A review of flow and heat transfer in cavities and their applications. Eur. Phys. J. Plus 136 (4), 353. http://dx.doi.org/10.1140/epjp/s13360-021-01320-3.

Khanafer, K., Vafai, K., Lightstone, M., 2003. Buoyancy-driven heat transfer enhancement in a two-dimensional enclosure utilizing nanofluids. Int. J. Heat Mass Transfer 46 (19), 3639–3653. http://dx.doi.org/10.1016/S0017-9310(03)00156-X.

Lawrence, J., Kumar, A.V., 2021. MHD natural convection of hybrid nanofluid in a porous cavity heated with a sinusoidal temperature distribution. Comput. Therm. Sci.: Int. J. 13 (5), http://dx.doi.org/10.1615/ComputThermalScien.2021037663.

Li, H., Cui, Q., Feng, B., Wang, J., Lu, X., Weng, J., 2013. Antibacterial activity of $TiO_2$ nanotubes: Influence of crystal phase, morphology and Ag deposition. Appl. Surf. Sci. 284, 179–183. http://dx.doi.org/10.1016/j.apsusc.2013.07.076.

Li, W., Wang, Y., Zou, C., 2020. Stability, thermal conductivity and supercooling behavior of novel $\beta$–CD–$TiO_2$–Ag cooling medium-based nanofluids for eco-friendly cold thermal energy storage. J. Clean. Prod. 259, 121162. http://dx.doi.org/10.1016/j.jclepro.2020.121162.

Mansour, M., Mahdy, A., Ahmed, S., 2020. An inclined MHD mixed radiative–convection flow of a micropolar hybrid nanofluid within a lid–driven inclined odd–shaped cavity. Phys. Scr. 96 (2), 025705. http://dx.doi.org/10.1088/1402-4896/abd1b0.

Mirzaei, A., Jalili, P., Afifi, M.D., Jalili, B., Ganji, D.D., 2023. Convection heat transfer of MHD fluid flow in the circular cavity with various obstacles: Finite element approach. Int. J. Thermofluids 20, 100522. http://dx.doi.org/10.1016/j.ijft.2023.100522.

Rashidi, M.M., Sadri, M., Sheremet, M.A., 2021. Numerical simulation of hybrid nanofluid mixed convection in a lid–driven square cavity with magnetic field using high–order compact scheme. Nanomaterials 11 (9), 2250. http://dx.doi.org/10.3390/nano11092250.

Reddy, P.S., Sreedevi, P., Reddy, V.N., 2022. Entropy generation and heat transfer analysis of magnetic nanofluid flow inside a square cavity filled with carbon nanotubes. Chem. Thermodyn. Therm. Anal. 6, 100045. http://dx.doi.org/10.1016/j.ctta.2022.100045.

Roy, N.C., 2022. MHD natural convection of a hybrid nanofluid in an enclosure with multiple heat sources. Alex. Eng. J. 61 (2), 1679–1694. http://dx.doi.org/10.1016/j.aej.2021.06.076.

Saha, T., Islam, T., Yeasmin, S., Parveen, N., 2023. Thermal influence of heated fin on MHD natural convection flow of nanofluids inside a wavy square cavity. Int. J. Thermofluids 18, 100338. http://dx.doi.org/10.1016/j.ijft.2023.100338.

Sajjadi, H., Delouei, A.A., Atashafrooz, M., Sheikholeslami, M., 2018. Double MRT lattice Boltzmann simulation of 3-D MHD natural convection in a cubic cavity with sinusoidal temperature distribution utilizing nanofluid. Int. J. Heat Mass Transfer 126, 489–503. http://dx.doi.org/10.1016/j.ijheatmasstransfer.2018.05.064.

Sanzone, G., Zimbone, M., Cacciato, G., Ruffino, F., Carles, R., Privitera, V., Grimaldi, M., 2018. Ag/$TiO_2$ nanocomposite for visible light-driven photocatalysis. Superlattices Microstruct. 123, 394–402. http://dx.doi.org/10.1016/j.spmi.2018.09.028.

Scott, T.O., Ewim, D.R., Eloka-Eboka, A.C., 2022. Experimental investigation of natural convection $Al_2O_3$-MWCNT/water hybrid nanofluids inside a square cavity. Exp. Heat Transfer 1–19. http://dx.doi.org/10.1080/08916152.2022.2136284.

Selimefendigil, F., Chamkha, A.J., 2021. MHD mixed convection of Ag–MgO/water nanofluid in a triangular shape partitioned lid-driven square cavity involving a porous compound. J. Therm. Anal. Calorim. 143 (2), 1467–1484. http://dx.doi.org/10.1007/s10973-020-09472-7.

Seo, J., Ryu, D., 2023. HOW–MHD: A high–order WENO–based magnetohydrodynamic code with a high–order constrained transport algorithm for astrophysical applications. http://dx.doi.org/10.3847/1538-4357/acdf4b, arXiv preprint arXiv:2304.04360.

Sivasankaran, S., Bhuvaneswari, M., Alzahrani, A., 2020. Numerical simulation on convection of non–Newtonian fluid in a porous enclosure with non–uniform heating and thermal radiation. Alex. Eng. J. 59 (5), 3315–3323. http://dx.doi.org/10.1016/j.aej.2020.04.045.

Soylu, S.K., Acar, Z.Y., Asiltürk, M., Atmaca, İ., 2022. Effects of doping on the thermophysical properties of Ag and Cu doped $TiO_2$ nanoparticles and their nanofluids. J. Mol. Liq. 368, 120615. http://dx.doi.org/10.1016/j.molliq.2022.120615.

Tasnim, S., Mitra, A., Saha, H., Islam, M.Q., Saha, S., 2023. MHD conjugate natural convection and entropy generation of a nanofluid filled square enclosure with multiple heat-generating elements in the presence of Joule heating. Results Eng. 17, 100993. http://dx.doi.org/10.1016/j.rineng.2023.100993.

Tayebi, T., Chamkha, A.J., 2020. Entropy generation analysis due to MHD natural convection flow in a cavity occupied with hybrid nanofluid and equipped with a conducting hollow cylinder. J. Therm. Anal. Calorim. 139 (3), 2165–2179. http://dx.doi.org/10.1007/s10973-019-08651-5.

Thirumalaisamy, K., Reddy, A.S., 2023. Numerical computation on MHD natural convective ternary nanofluid flow and heat transfer in a porous square cavity: Marker-and-cell technique. Internat. J. Numer. Methods Heat Fluid Flow 33 (10), 3425–3466. http://dx.doi.org/10.1108/HFF-04-2023-0167.

Turkyilmazoglu, M., 2022a. Driven flow motion by a dually moving lid of a square cavity. Eur. J. Mech. B Fluids 94, 17–28. http://dx.doi.org/10.1016/j.euromechflu.2022.02.005.

Turkyilmazoglu, M., 2022b. Exponential nonuniform wall heating of a square cavity and natural convection. Chinese J. Phys. 77, 2122–2135. http://dx.doi.org/10.1016/j.cjph.2021.12.021.

Yu, B., Leung, K.M., Guo, Q., Lau, W.M., Yang, J., 2011. Synthesis of Ag–$TiO_2$ composite nano thin film for antimicrobial application. Nanotechnology 22 (11), 115603. http://dx.doi.org/10.1088/0957-4484/22/11/115603.